Electronic Supplementary Information

Water soluble macrocyclic host for recognition of *N*-methylquinolinium salts in water

Yuan-Hong Tian,[a] Han Qin, [a] Man-Hua Ding,*[,a] Lin-Li Tang, [a] Fei Zeng*[,a]

[a]Department of Biology and Chemistry, Hunan University of Science and Engineering, Yongzhou 425199, China.

E-mail: zengfei@iccas.ac.cn*; dingxiaolove@126.com*

Contents

1. Materials and Methods.

All reactions were carried out with oven-dried glassware. Commercial reagents were used without further purification. Flash column chromatography was performed on 100-200 mesh silica gel. ^{1}H NMR, ^{13}C NMR spectra were recorded on a Bruker DMX400 NMR spectrometer. Melting points were determined using WRR melting point apparatus and were uncorrected. High Resolution atmospheric-pressure chemical ionization mass spectra (APCI-MS) were determined by Bruker Daltonics. Inc, APEX II. FT-ICRMS. Electrospray ionization mass spectra (ESI-MS) were recorded on the Thermo Fisher® Exactive LC-MS spectrometer.

2. Synthesis of New Compounds.

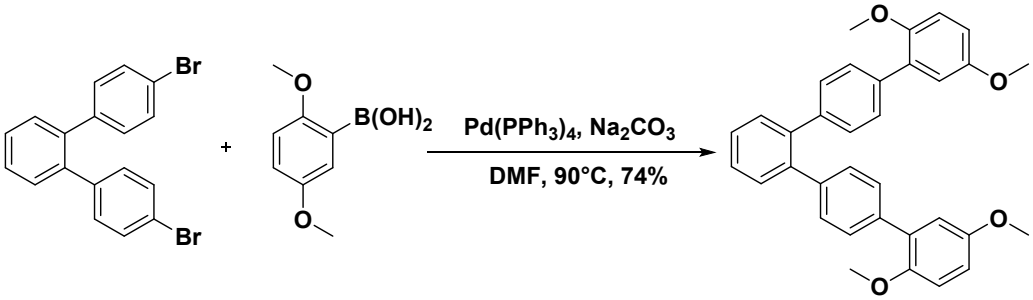

4

Compound 4: A mixture of 4,4"-dibromo-1,1':2',1"-terphenyl (3.86 g, 10 mmol), Na_2CO_3 (2.96 g, 28 mmol), 2,4-dimethoxyphenylboronic acid (4.00 g, 22 mmol), and catalytic amount of CuI (21 mg) and tetrakis(triphenylphosphine)- palladium (320 mg) in 100 mL DMF in a flask was stirred at 90 ^{o}C for 24 h under N_2. After evaporating the solvents, resulting mixture was extracted with dichloromethane (3 × 50 mL) and then washed with water and brine successively. The organic layer was dried over anhydrous Na_2SO_4 and evaporated. The residue was purified by column chromatography on silica gel with dichloromethane/ Petroleum ether as eluent (4:1) to afford compound **4** (3.74 g, yield 74%) as a white solid. ^{1}H NMR (400 MHz, Chloroform-*d*) δ 7.43 (dd, *J* = 5.4, 3.5 Hz, 2H), 7.36 (d, *J* = 8.3 Hz, 6H), 7.18 (d, *J* = 2.6 Hz, 4H), 6.85 – 6.81 (m, 4H), 6.75 (dd, *J* = 8.9, 2.9 Hz, 2H), 3.72 (s, 6H), 3.66 (s, 6H). ^{13}C NMR (101 MHz, $CDCl_3$) δ 153.9, 150.9, 140.4, 140.3, 136.5, 131.4, 130.8,

129.6, 129.0, 127.5, 116.6, 113.1, 113.0, 56.5, 55.8. HRMS (APCI) m/z: $[M+H]^+$ calcd for $C_{34}H_{31}O_4$, 503.2222; found, 503.2228.

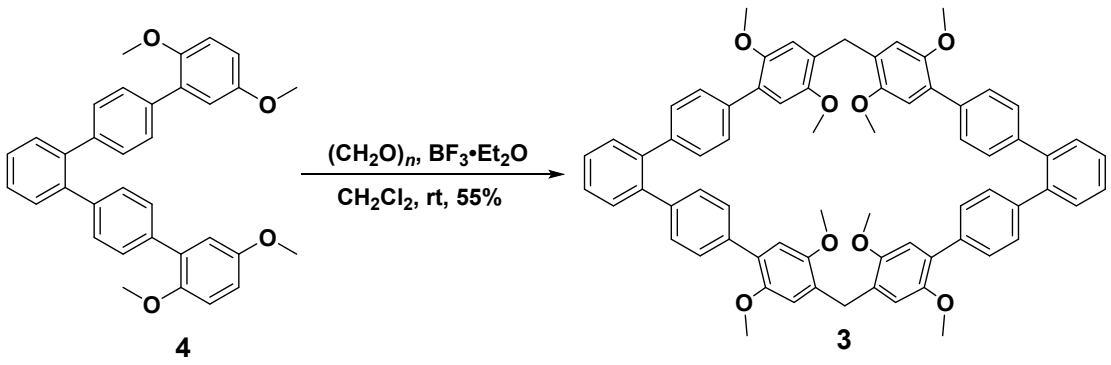

Compound 3: To a mixture of **4** (1.00 g, 2.0 mmol) and paraformaldehyde (180 mg, 6.0 mmol) in dichloromethane (150 mL) was added boron trifluoride diethyl etherate (0.3 mL, 2.4 mmol). The mixture was stirred at room temperature for 0.5 h. Then the reaction was quenched by the addition of 150 mL water. The organic layer was separated and dried with anhydrous $MgSO_4$. The solvent was removed in vacuo and the residue was separated by column chromatography on silica gel (eluent: 2:1 DCM/Petroleum ether) to give **3** (566 mg, 55%) as a white solid. ^{1}H NMR (400 MHz, Chloroform-*d*) δ 7.46 (dd, *J* = 5.5, 3.5 Hz, 4H), 7.39 – 7.34 (m, 12H), 7.12 (d, *J* = 8.1 Hz, 8H), 6.82 (s, 4H), 6.65 (s, 4H), 3.90 (s, 4H), 3.76 (s, 12H), 3.47 (s, 12H).^{13}C NMR (101 MHz, $CDCl_3$) δ 152.2, 150.6, 140.5, 139.9, 136.7, 130.4, 129.7, 129.0, 128.8, 127.6, 116.4, 112.9, 57.2, 56.1, 30.1. HRMS (APCI) m/z: $[M+H]^+$ calcd for $C_{70}H_{61}O_8$, 1029.4366; found, 1029.4365.

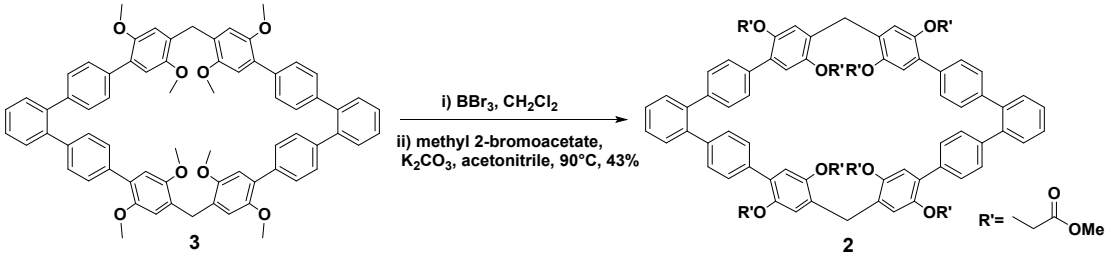

Compound 2: Dry CH_2Cl_2 (250 mL) was added into a flask. Then compound **3** (3.09 g, 3 mmol) was added tardily in an ice bath. After 30 min, tribromoborane (5 mL, 50 mmol) was added into the reaction flask. Upon stirring at room temperature for overnight, the mixture was quenched with water. After stirring the reaction mixture

for 6 h, product **3**-OH was obtained by filtration and used in the next step without further purification. **3**-OH (1.83 g, 2 mmol) and Na_2CO_3 (4.42 g, 32 mmol) were dissolved in acetonitrile (200 mL). And Methyl bromoacetate (10 mL, 90 mM) was added at room temperature. Then the mixture was heated at 90 °C in an oil bath for 72 h. After cooling to room temperature, the mixture was quenched with water. The organic layer was collected and concentrated, and product **2** (white solid, 1.28 g, 43%) was afforded by column chromatography (petroleum ether/dichloromethane = 2/1, v/v). ^{1}H NMR (400 MHz, Chloroform-*d*) δ 7.42 – 7.35 (m, 16H), 7.16 (d, *J* = 8.0 Hz, 8H), 6.96 (s, 4H), 6.68 (s, 4H), 4.56 (s, 8H), 4.38 (s, 8H), 4.01 (s, 4H), 3.68 (s, 12H), 3.48 (s, 12H). ^{13}C NMR (101 MHz, $CDCl_3$) δ 169.7, 169.5, 150.9, 149.6, 140.3, 140.1, 136.1, 130.9, 129.7, 129.0, 127.6, 117.8, 114.4, 66.7, 66.2, 52.1, 51.8. HRMS (APCI) m/z: $[M+H]^+$ calcd for $C_{86}H_{77}O_{24}$, 1493.4805; found, 1493.4815.

Compound 3-OH**:** ^{1}H NMR (400 MHz, Acetone-d_6) δ 8.06 (s, 4H), 7.80 (s, 4H), 7.51 (dd, *J* = 13.2, 5.8 Hz, 16H), 7.18 (d, *J* = 8.1 Hz, 8H), 6.91 (s, 4H), 6.65 (s, 4H), 3.86 (s, 4H). ^{13}C NMR (101 MHz, Acetone) δ 148.0, 147.3, 140.4, 136.9, 130.4, 129.3, 128.6, 127.5, 125.8, 118.0, 116.2.

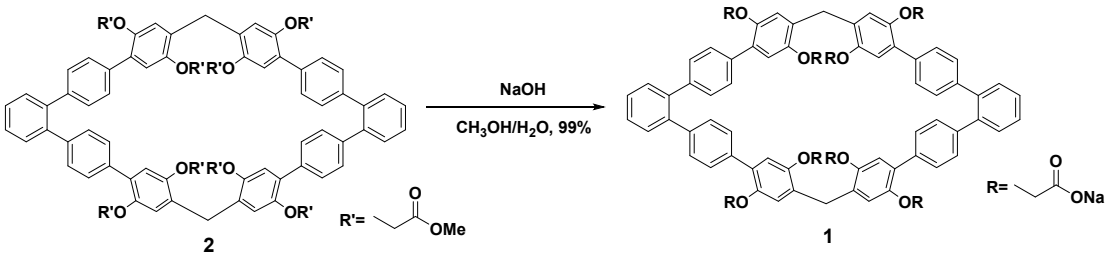

Compound 1: Compound **2** (1.49 g, 1 mmol) and NaOH (320 mg, 8 mmol) were added into 40 mL CH_3OH/H_2O= 9:1 (V/V). After stirred the reaction mixture at 90 °C for 20 h, host **1** (white solid, 1.53 g, 99%) was obtained by removing the sovlent under reduced pressure. ^{1}H NMR (400 MHz, D_2O) δ 7.49 (s, 16H), 7.29 (d, *J* = 7.9 Hz, 8H), 6.81 (s, 4H), 6.69 (s, 4H), 4.37 (s, 8H), 4.22 (s, 8H), 4.01 (s, 4H). ^{13}C NMR (101 MHz, D_2O) δ 177.1, 150.7, 149.2, 140.1, 136.4, 129.69, 129.3, 128.0, 115.3, 68.2. HRMS (APCI) m/z: $[M+H]^+$ calcd for $C_{78}H_{53}O_{24}Na_8$, 1557.2108; found, 1557.2111.

3. ^{1}H NMR and ^{13}C NMR Spectral of New compounds.

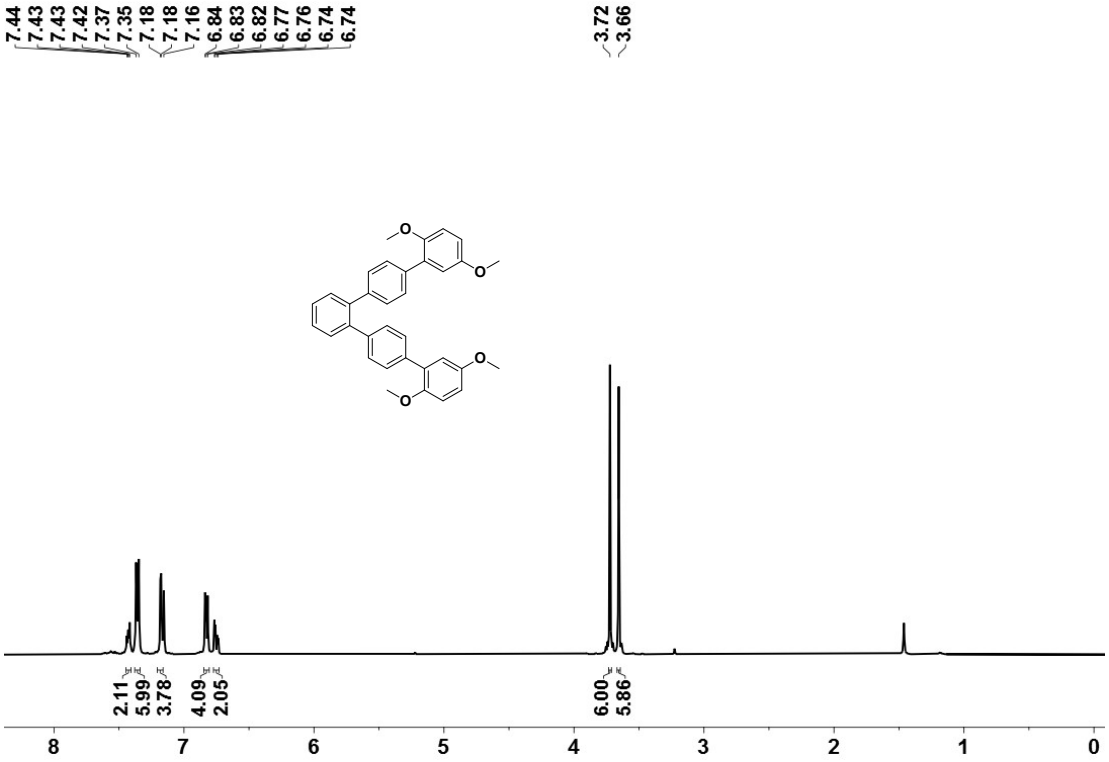

Figure S1.^{1}H NMR spectrum (400 MHz, $CDCl_3$, 298K) of **4**

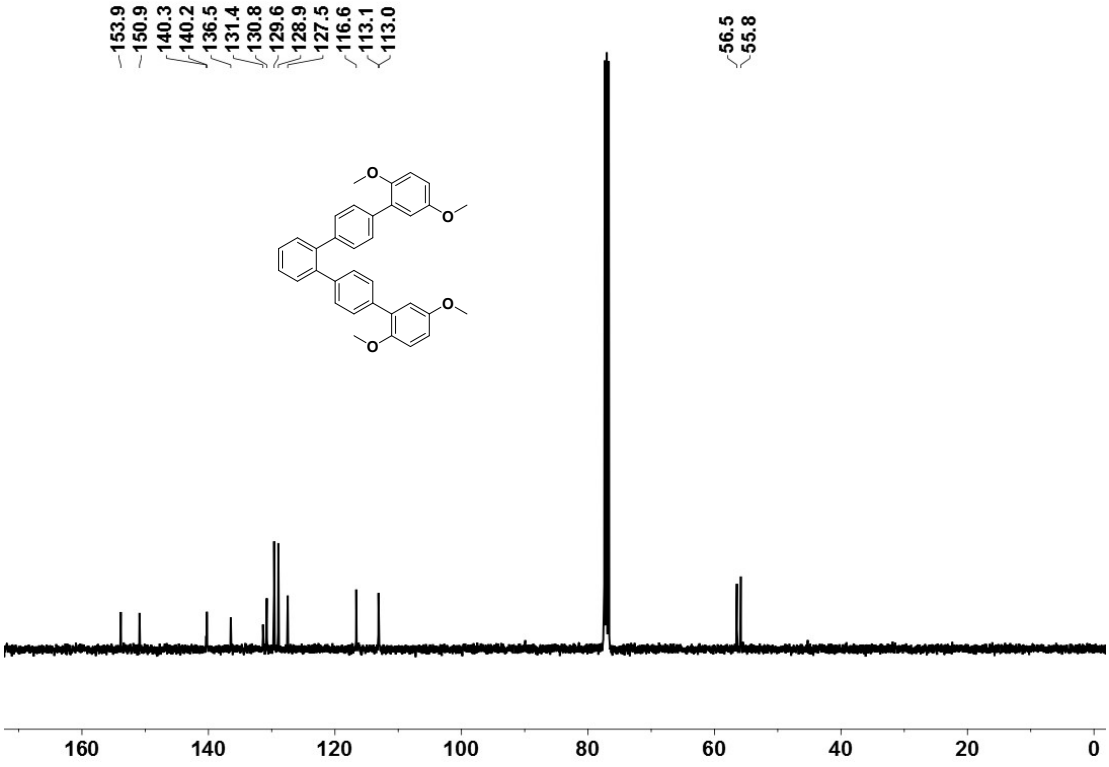

Figure S2.^{13}C NMR spectrum (101 MHz, $CDCl_3$, 298K) of **4**

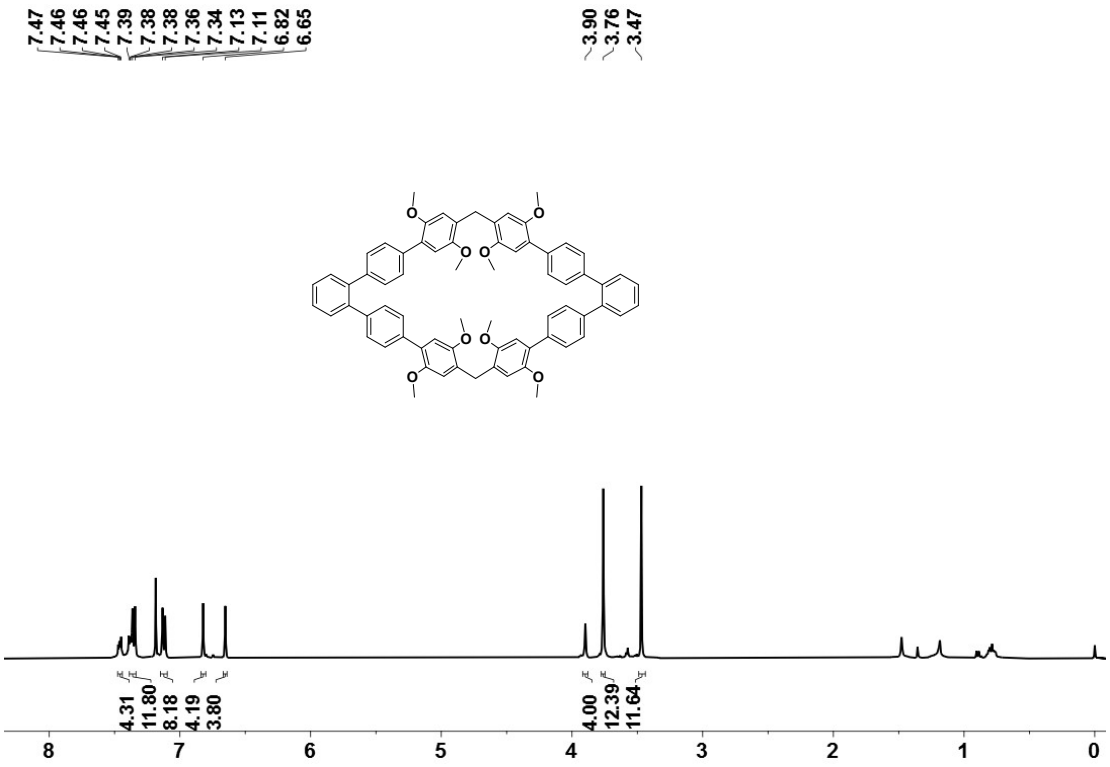

Figure S3.[1]H NMR spectrum (400 MHz, $CDCl_3$, 298K) of **3**

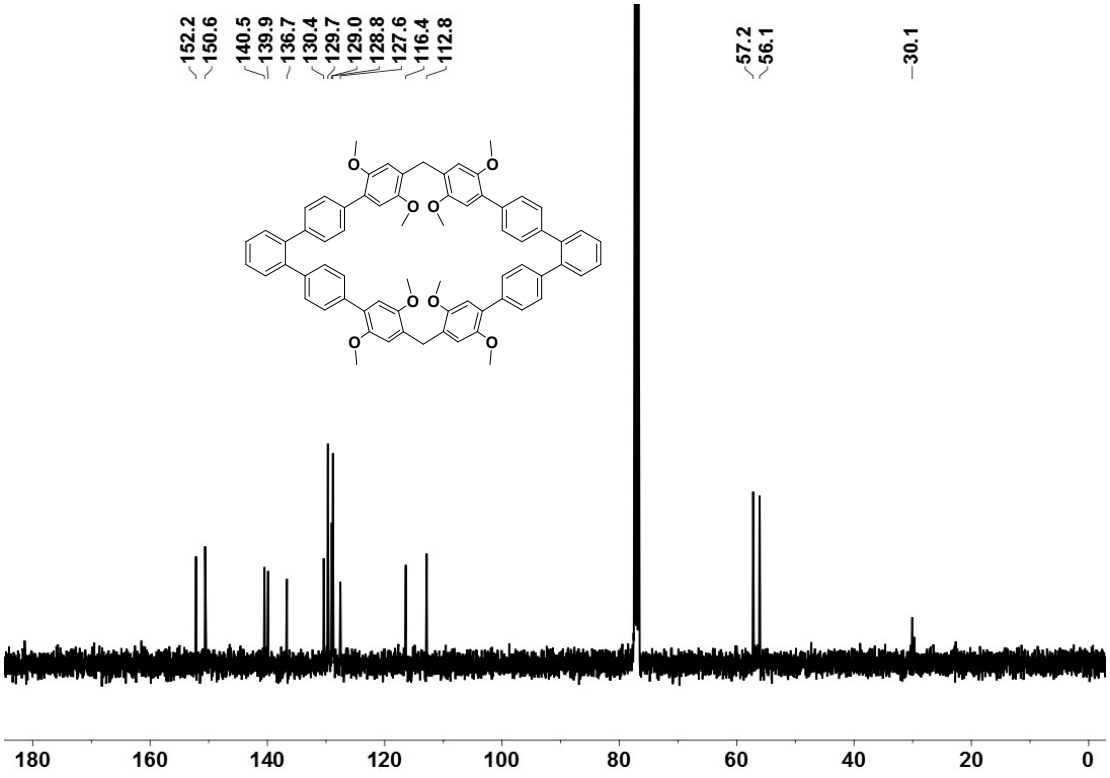

Figure S4.[13]C NMR spectrum (101 MHz, $CDCl_3$, 298K) of **3**

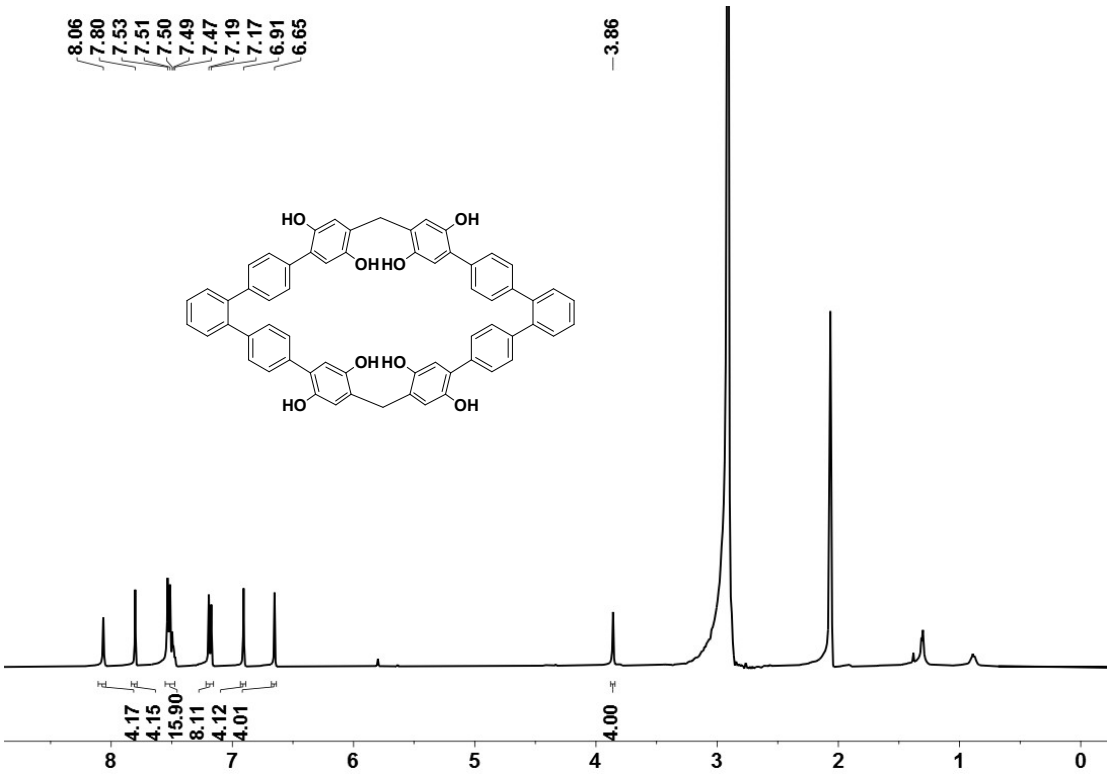

Figure S5.[1]H NMR spectrum (400 MHz, Acetone, 298K) of **3**-OH

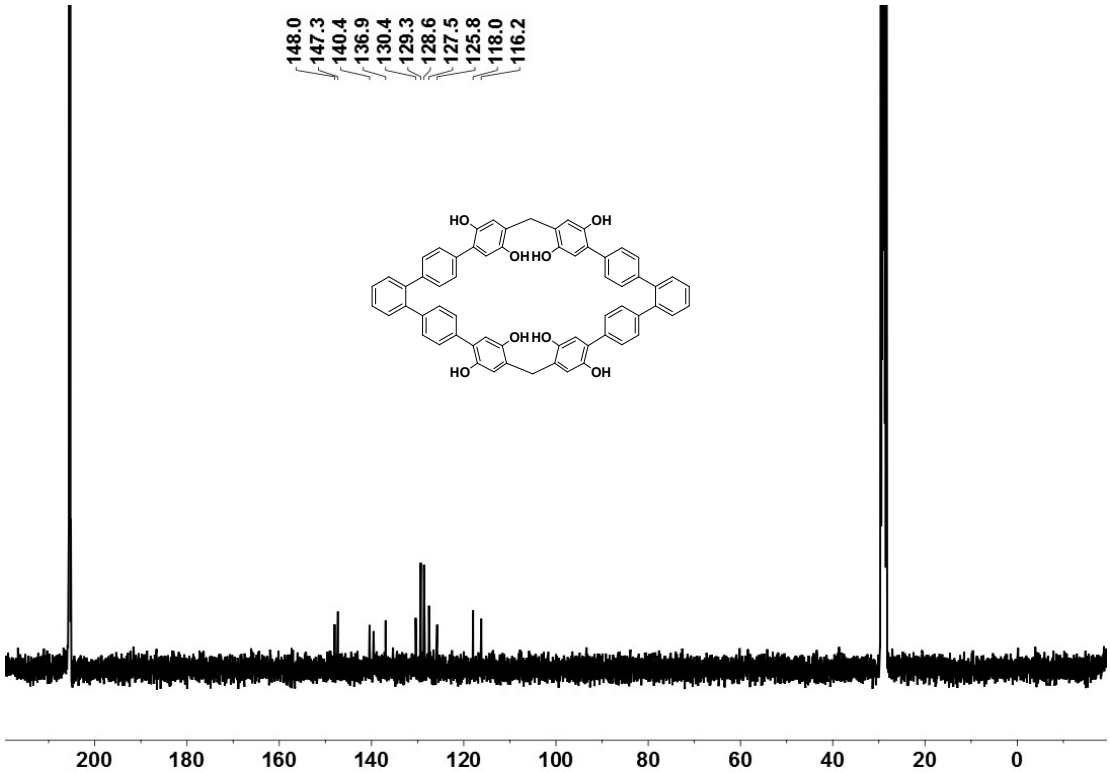

Figure S6.[13]C NMR spectrum (101 MHz, Acetone, 298K) of **3**-OH

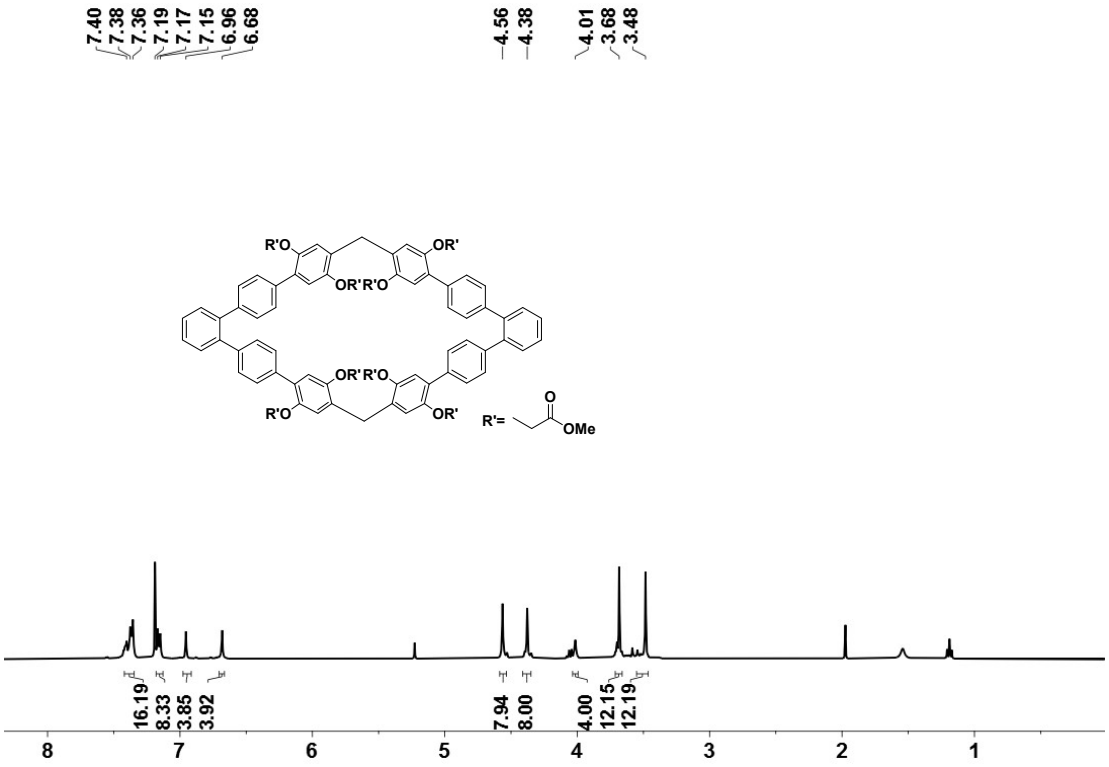

Figure S7.[1]H NMR spectrum (400 MHz, $CDCl_3$, 298K) of **2**

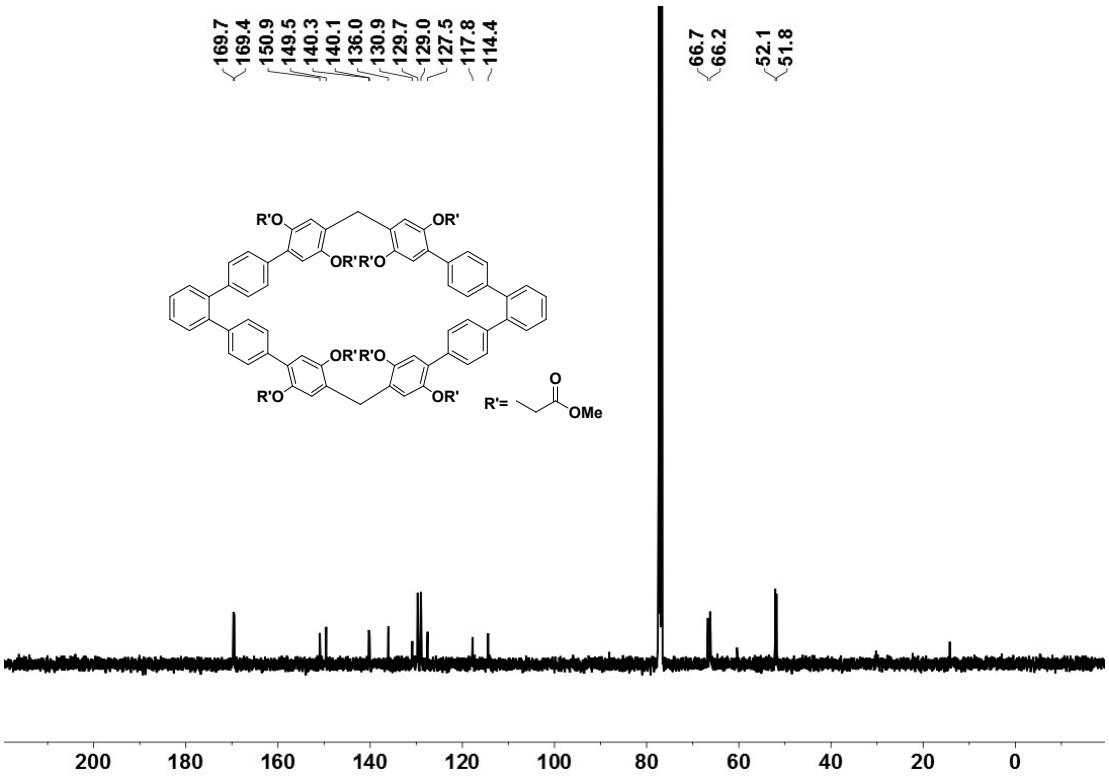

Figure S8.[13]C NMR spectrum (101 MHz, $CDCl_3$, 298K) of **2**

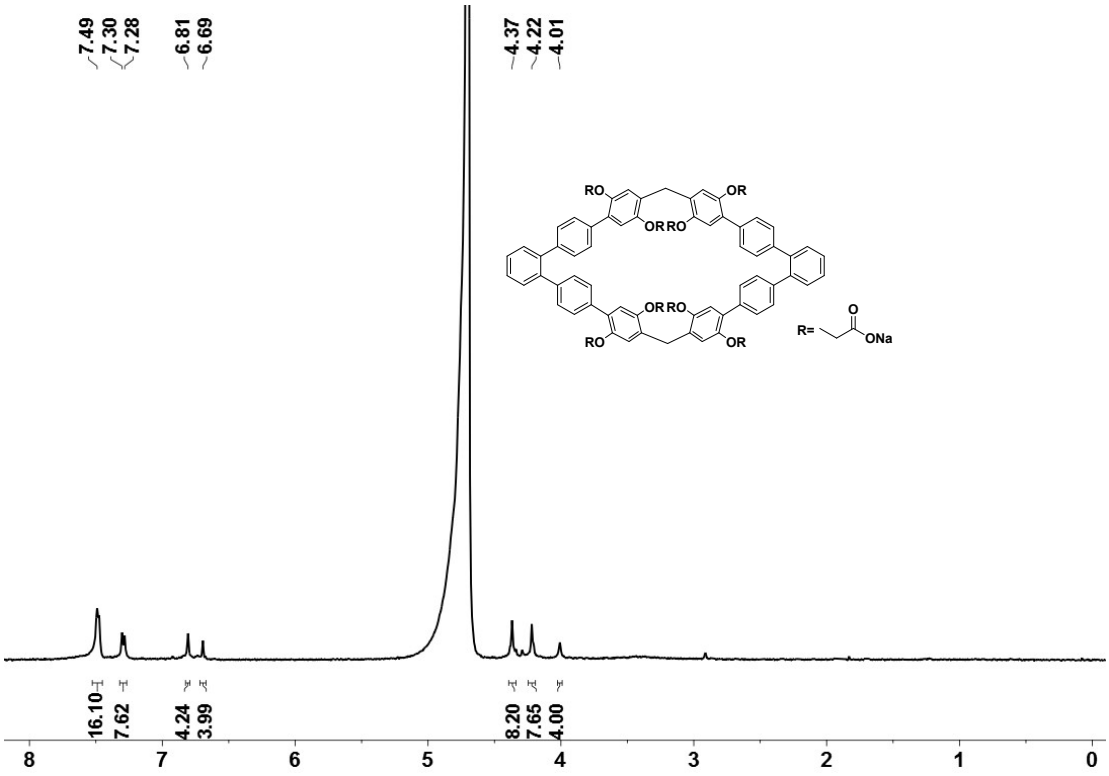

Figure S9.[1]H NMR spectrum (400 MHz, D_2O, 298K) of **1**

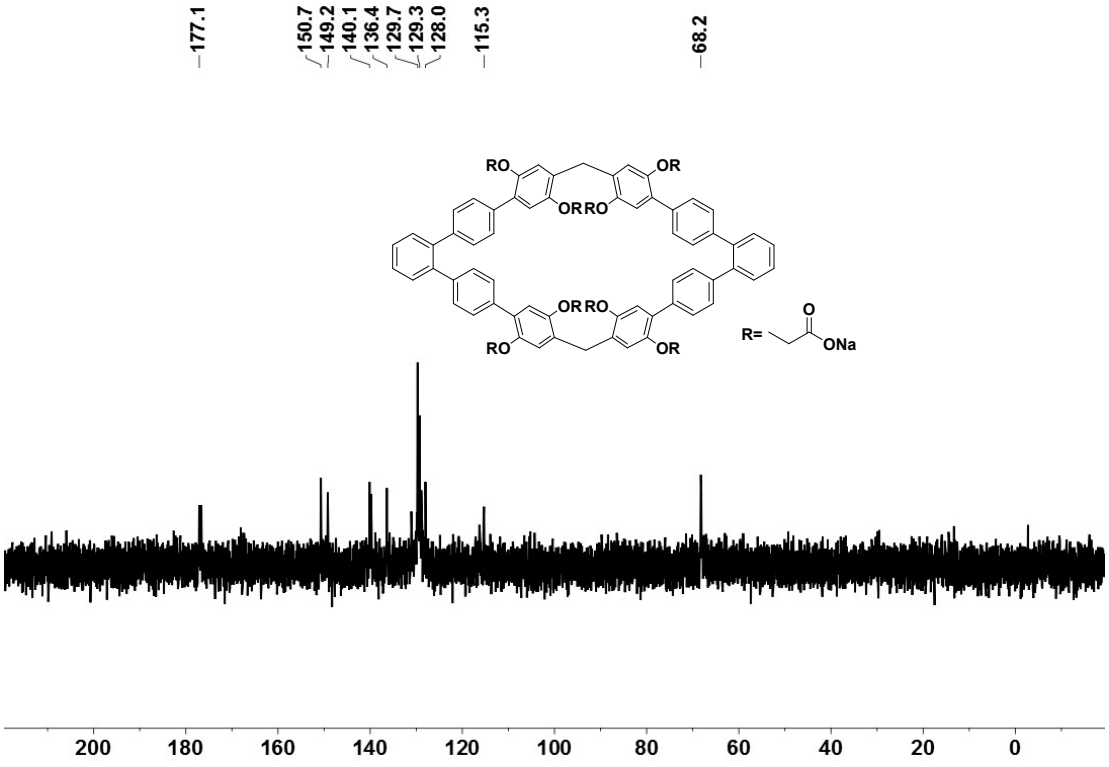

Figure S10.[13]C NMR spectrum (101 MHz, D_2O, 298K) of **1**

4. ^{1}H NMR studies of Complexation of the Host and Guest

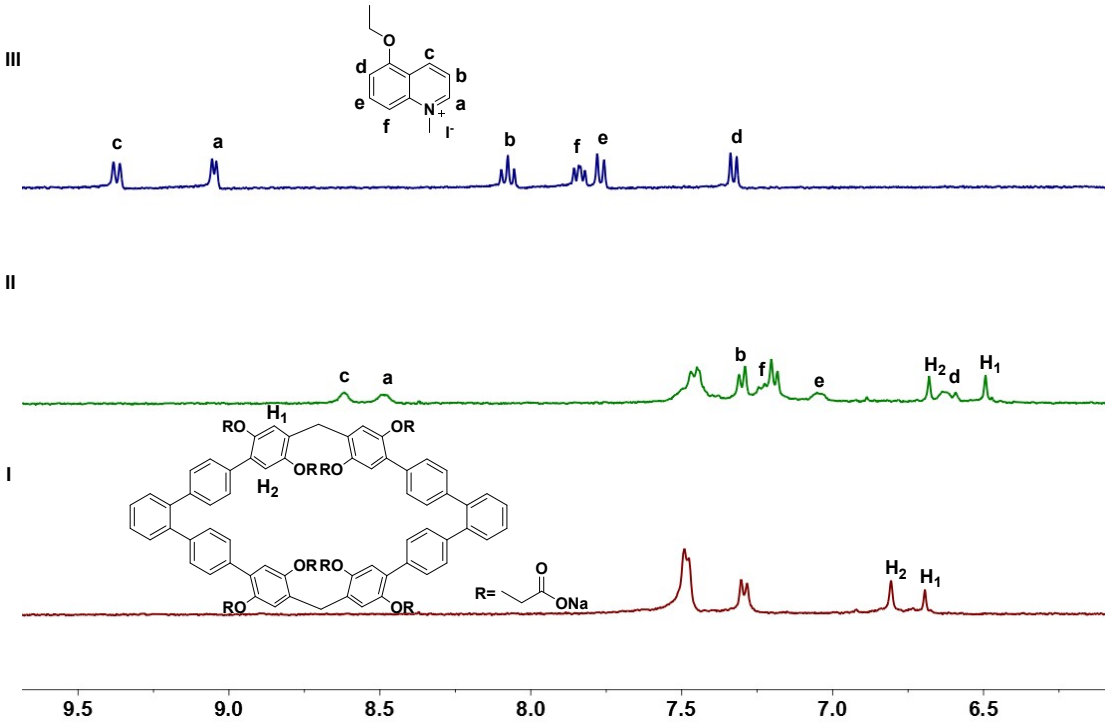

Figure S11. Partial ^{1}H NMR spectra (400 MHz, D_2O, 298 K) of (I) free **1**, (II) **1** and 1.0 equiv. of **G2**, and (III) free **G2**. $[\mathbf{1}]_0$ = 1.0 mM.

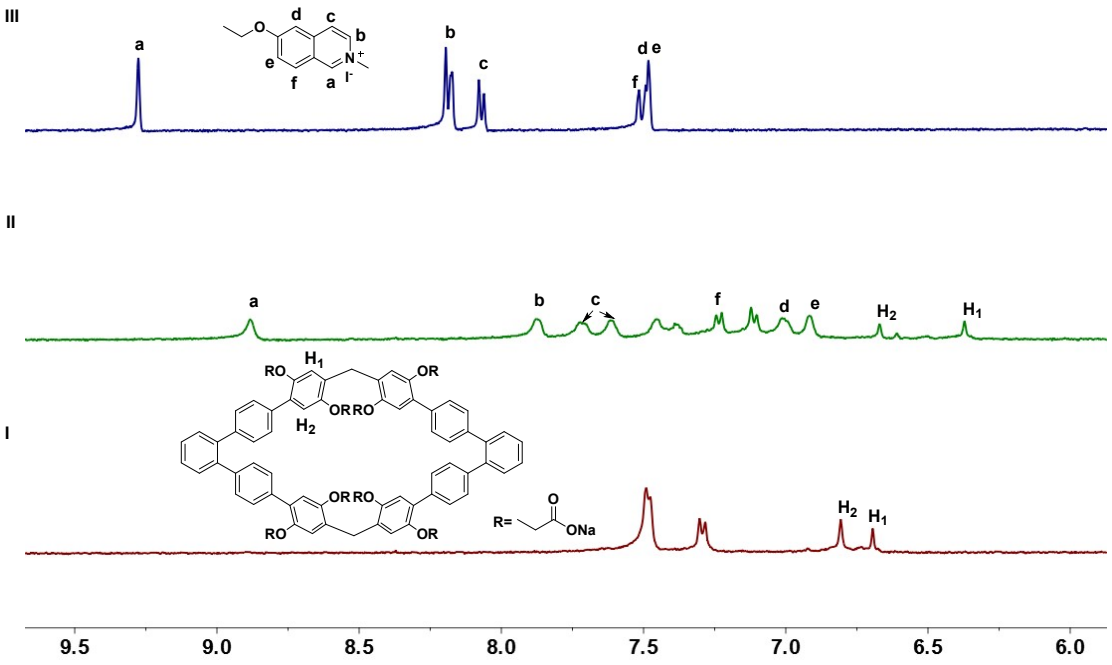

Figure S12 Partial ^{1}H NMR spectra (400 MHz, D_2O, 298 K) of (I) free **1**, (II) **1** and 1.0 equiv. of **G3**, and (III) free **G3**. $[\mathbf{1}]_0$ = 1.0 mM.

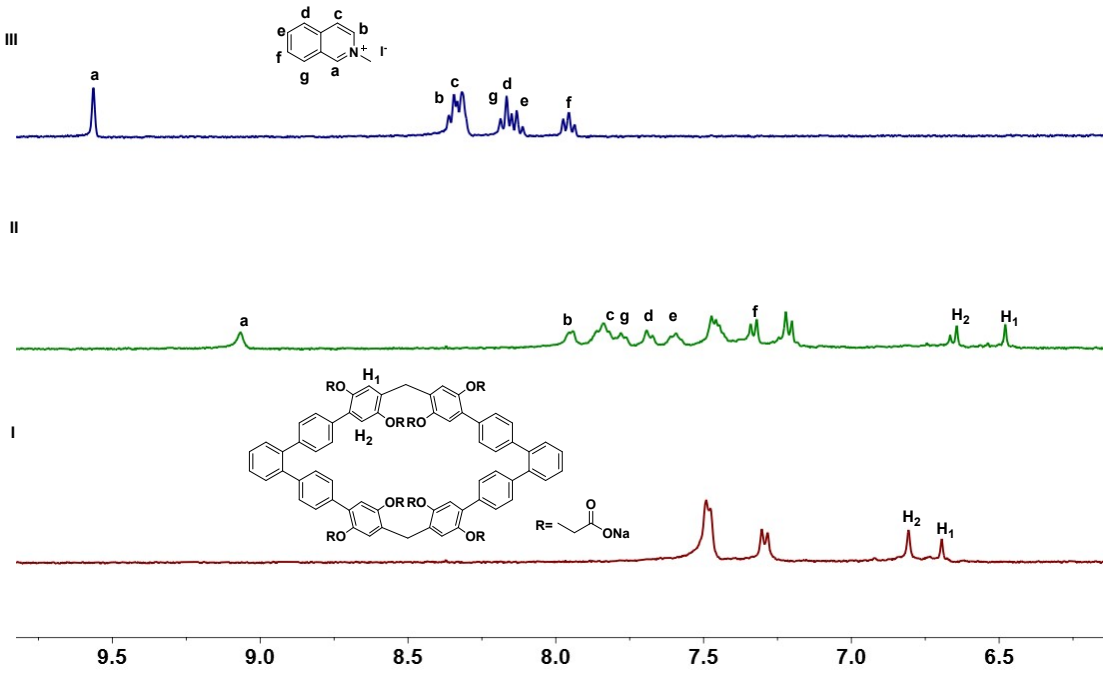

Figure S13 Partial ^{1}H NMR spectra (400 MHz, D_2O, 298 K) of (I) free **1**, (II) **1** and 1.0 equiv. of **G4**, and (III) free **G4**. $[\mathbf{1}]_0$ = 1.0 mM.

5. Determination of the Association Constants of the Complexes

In the ^{1}H NMR titrations, D_2O was chosen to dissolve the host and the guests. Chemical shifts were reported in parts per million (*ppm*). By a mole ratio plot, each stoichiometry was determined. Titration curve-fitting and association constant values were calculated by employing the BindFit program developed by Prof. Pall Thordarson of UNSW. 1:1 Binding stoichiometry was chosen in the BindFit program. This program employs a nonlinear least-squares regression analysis and is available free of cost online through the following link: http://supramolecular.org.

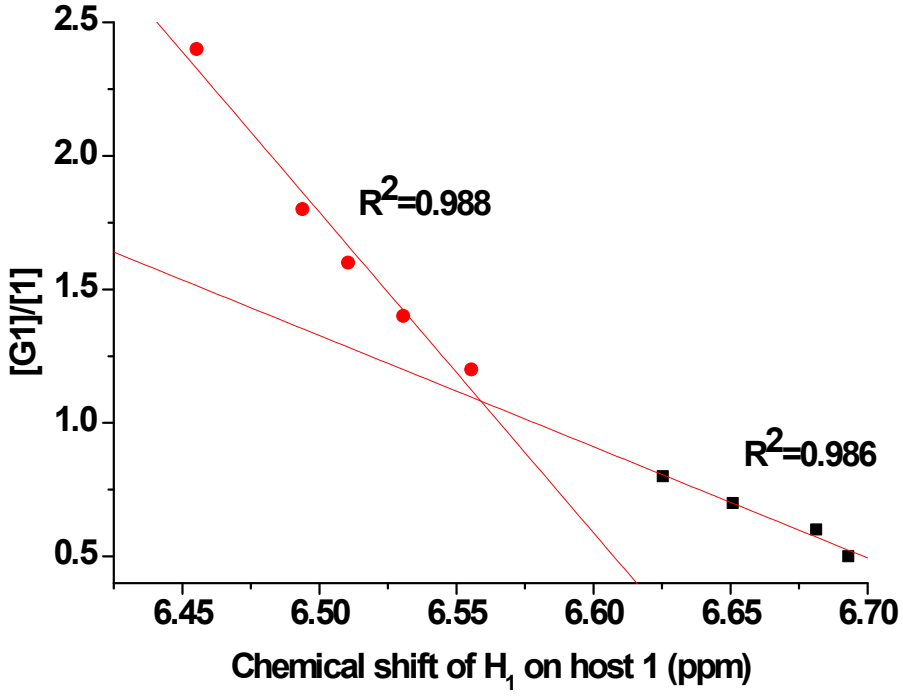

Figure S14. Mole ratio plot of the complexation of **1** and **G1** in D_2O at 298 K.

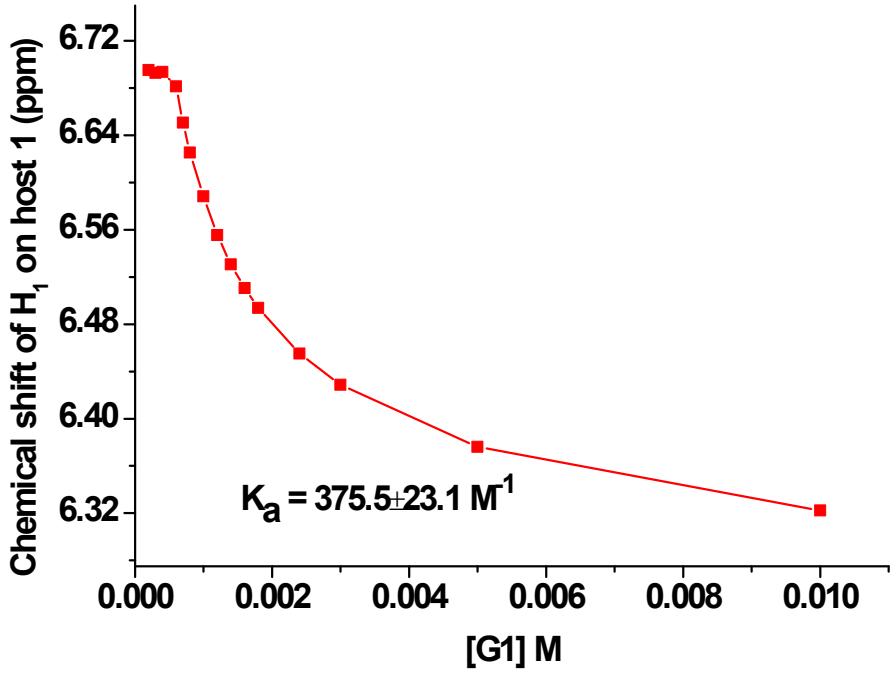

Figure S15. Plot of chemical shift (ppm) for the H_1 of **1** and **G1** in D_2O at 298 K.

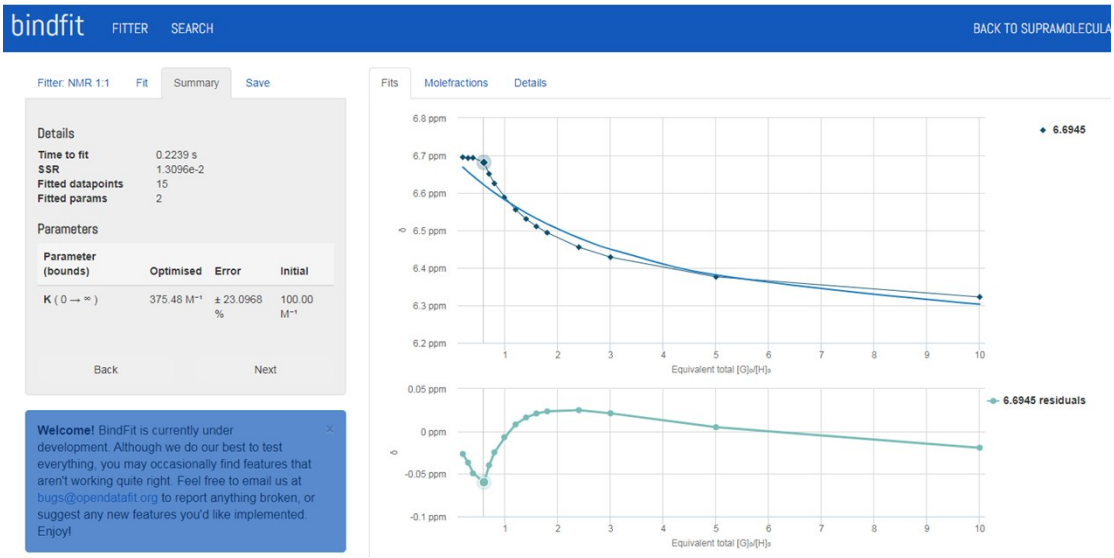

Figure S16. Nonlinear least-square analysis of the ^{1}H NMR binding data corresponding to the formation of **1@G1** complex. The data were fitted to a 1:1 binding model to give K_a = 375.5 ± 23.1 M^{-1}. The residual distribution is shown below the binding isotherm. All solid lines were obtained from non-linear curve-fitting to a 1:1 binding model using the www.supramolecular.org web applet.

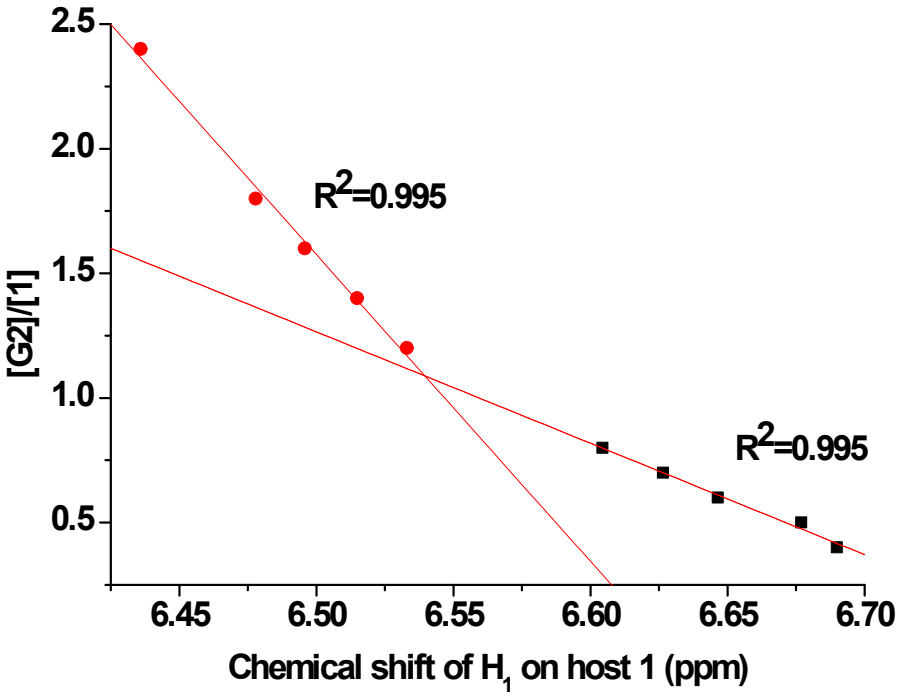

Figure S17. Mole ratio plot of the complexation of **1** and **G2** in D_2O at 298 K.

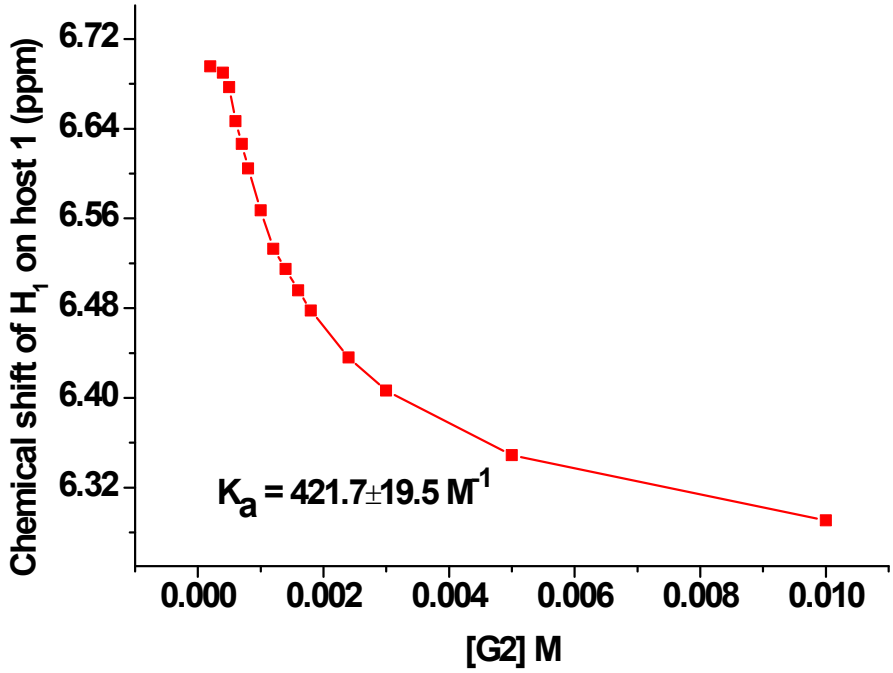

Figure S18. Plot of chemical shift (ppm) for the H_1 of **1** and **G2** in D_2O at 298 K.

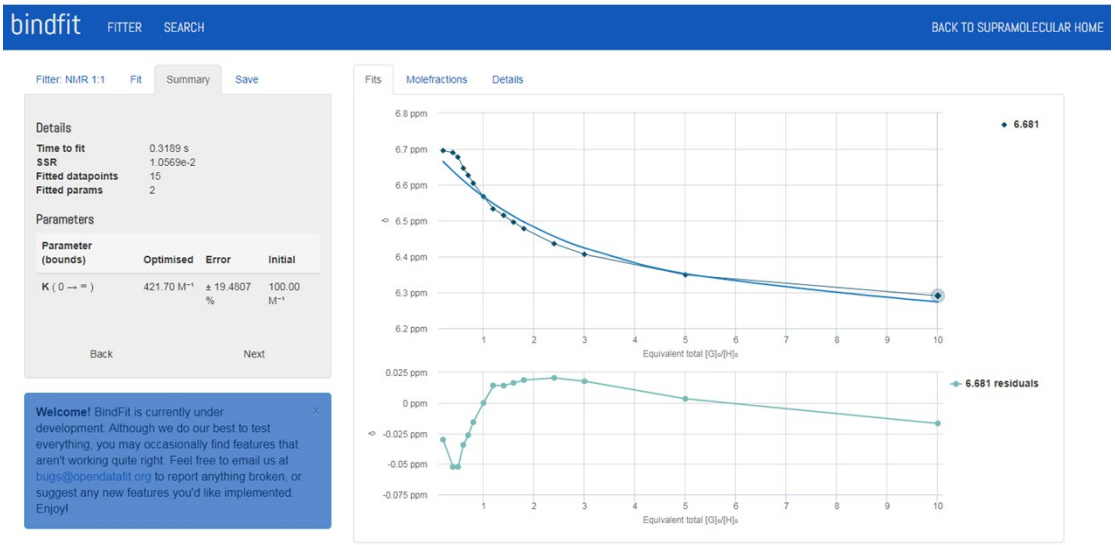

Figure S19. Nonlinear least-square analysis of the ^{1}H NMR binding data corresponding to the formation of **1@G2** complex. The data were fitted to a 1:1 binding model to give K_a = 421.7 ± 19.5 M^{-1}. The residual distribution is shown below the binding isotherm. All solid lines were obtained from non-linear curve-fitting to a 1:1 binding model using the www.supramolecular.org web applet.

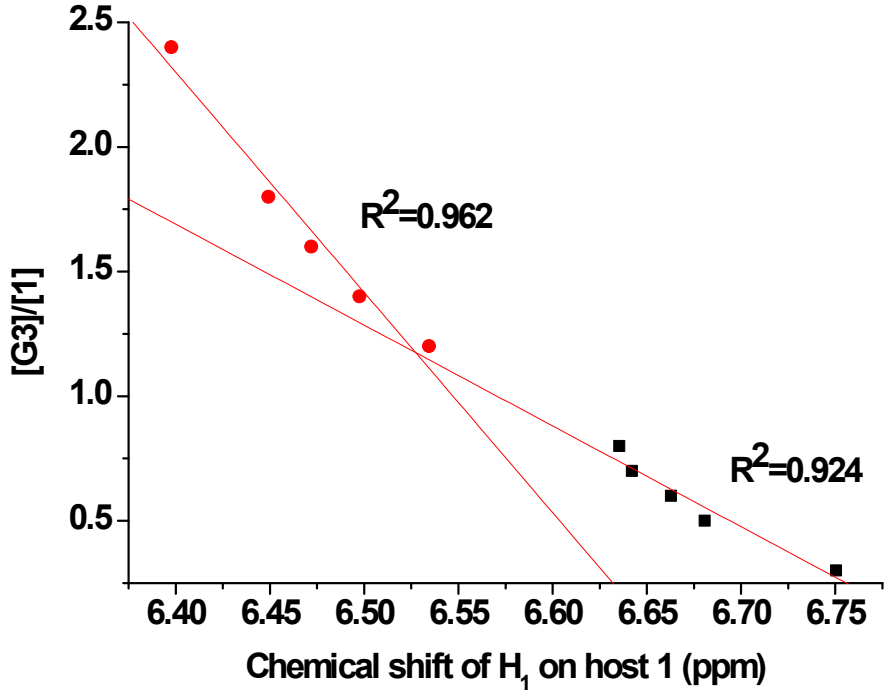

Figure S20. Mole ratio plot of the complexation of **1** and **G3** in D_2O at 298 K.

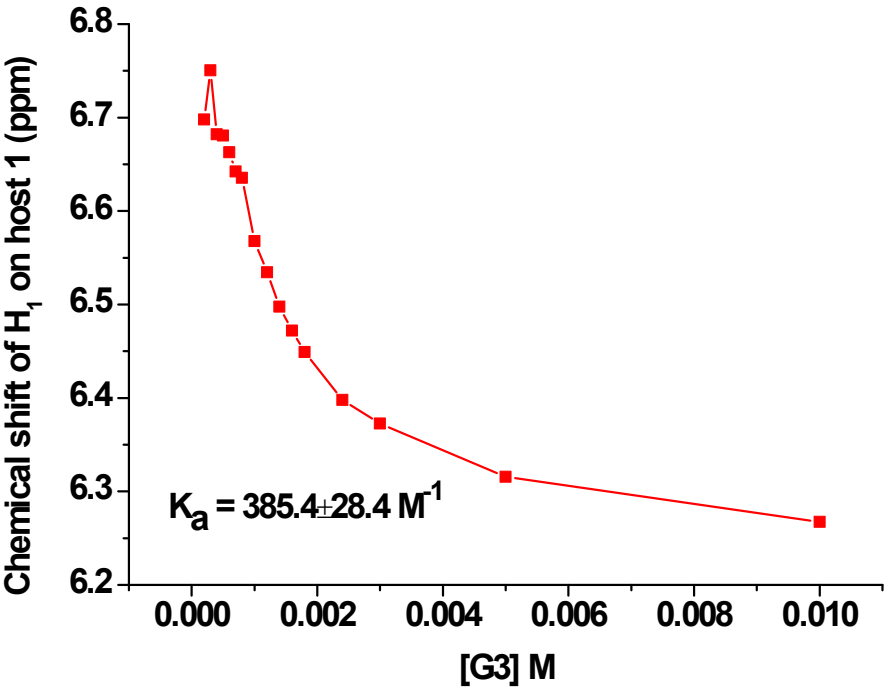

Figure S21. Plot of chemical shift (ppm) for the H_1 of **1** and **G3** in D_2O at 298 K.

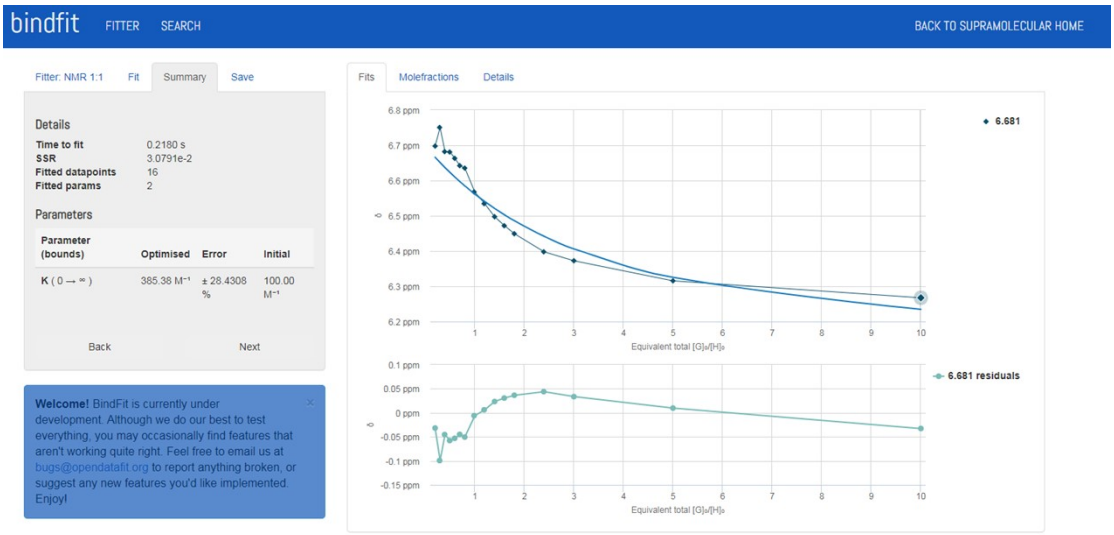

Figure S22. Nonlinear least-square analysis of the ^{1}H NMR binding data corresponding to the formation of **1@G3** complex. The data were fitted to a 1:1 binding model to give K_a = 385.4 ± 28.4 M^{-1}. The residual distribution is shown below the binding isotherm. All solid lines were obtained from non-linear curve-fitting to a 1:1 binding model using the www.supramolecular.org web applet.

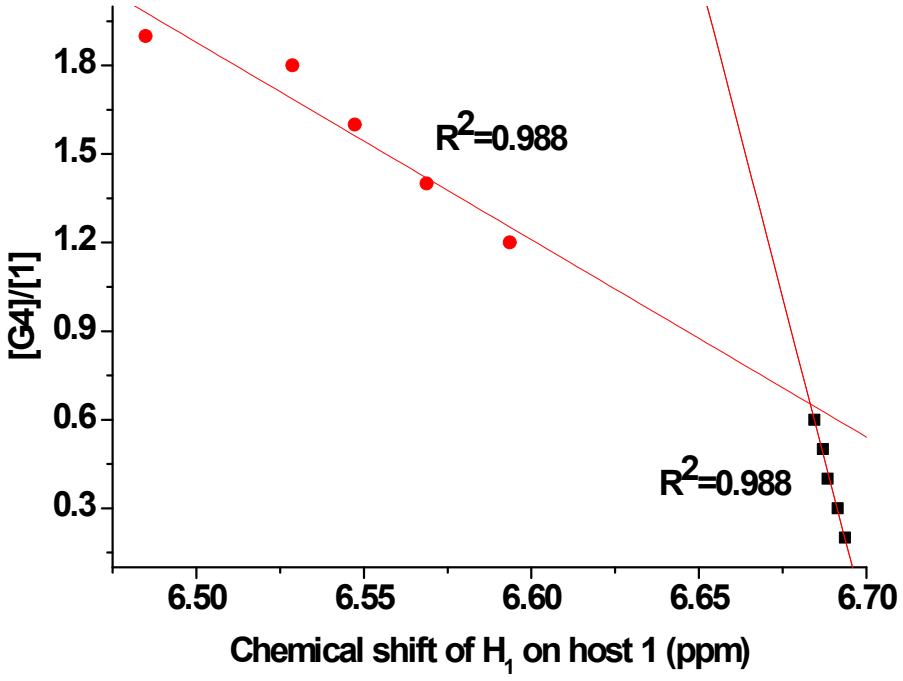

Figure S23. Mole ratio plot of the complexation of **1** and **G4** in D_2O at 298 K.

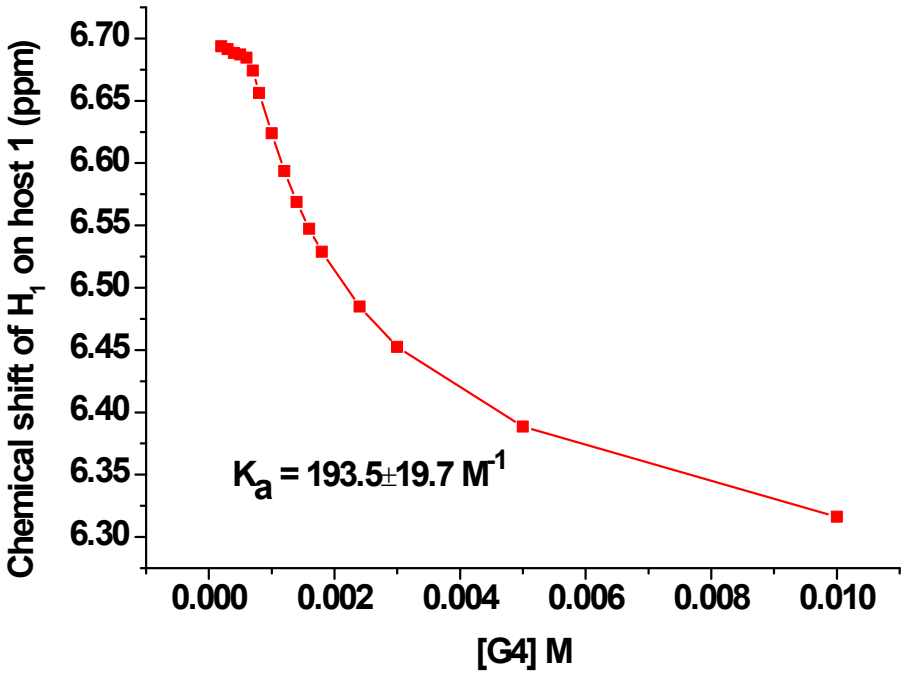

Figure S24. Plot of chemical shift (ppm) for the H_1 of **1** and **G4** in D_2O at 298 K.

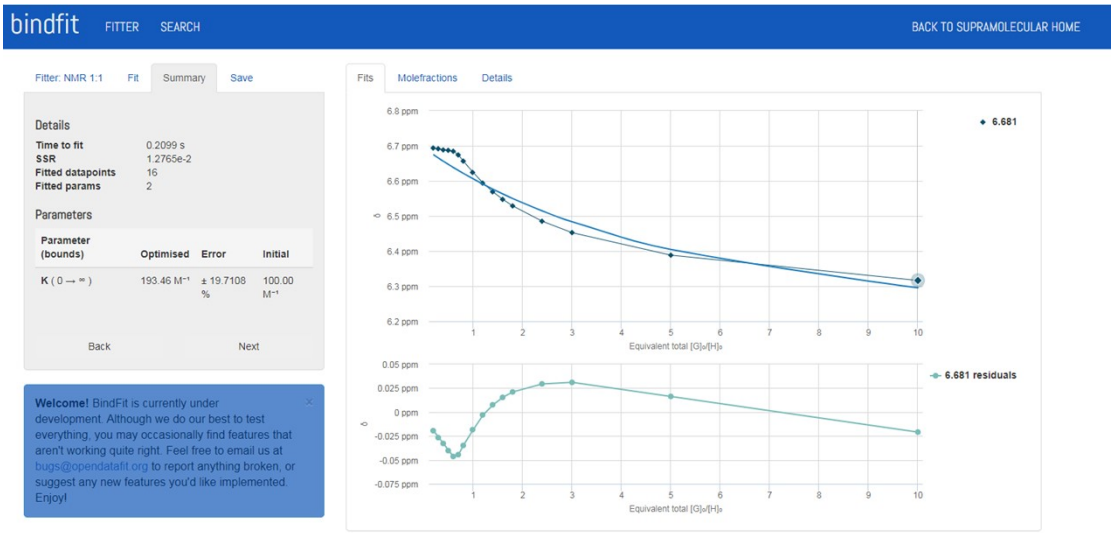

Figure S25. Nonlinear least-square analysis of the ^{1}H NMR binding data corresponding to the formation of **1@G4** complex. The data were fitted to a 1:1 binding model to give K_a = 193.5 ± 19.7 M^{-1}. The residual distribution is shown below the binding isotherm. All solid lines were obtained from non-linear curve-fitting to a 1:1 binding model using the www.supramolecular.org web applet.

6. Acid/base controlled complexation and decomplexation of **1@G2**, **1@G3** and **1@G4**

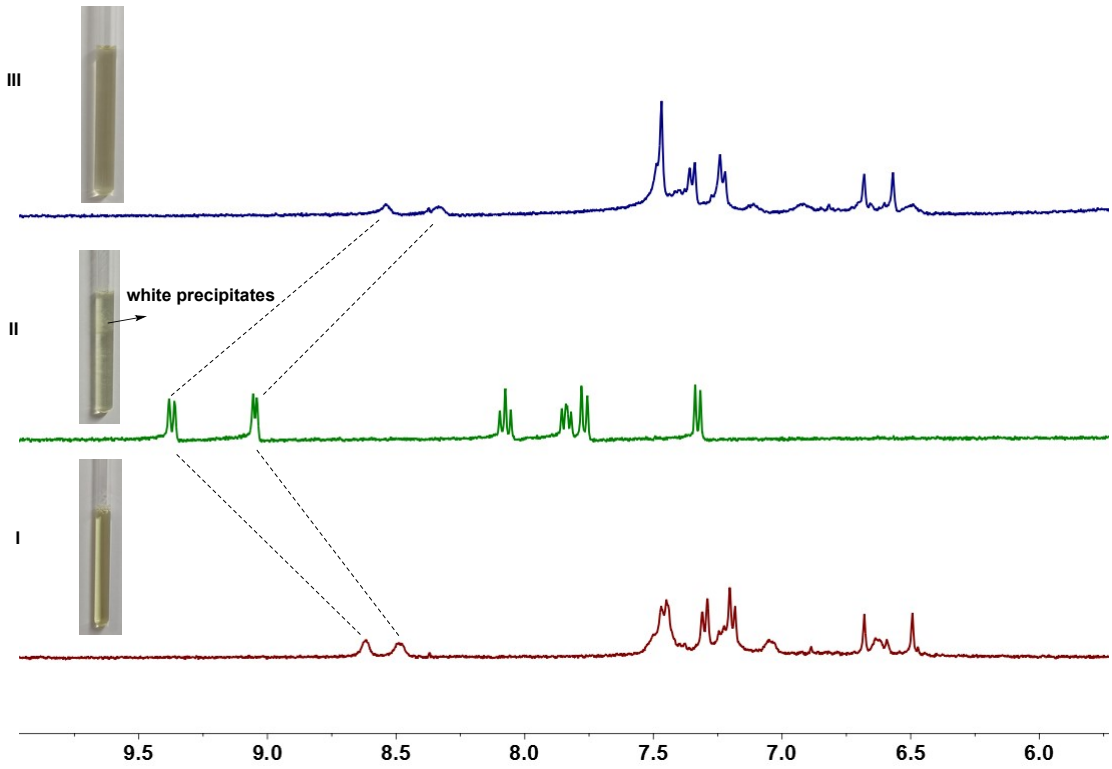

Figure S26. Partial ^{1}H NMR spectra (400 MHz, D_2O, 295 K) and photographs of (I) **1** and 1.0 equiv of **G2**, (b) after addition of 2.0 μL of aqueous DCl solution (20 wt%) to I, and (III) after addition of 1.0 μL of aqueous NaOD solution (40 wt%) to II. $[\mathbf{1}]_0$ = 1.0 mM.

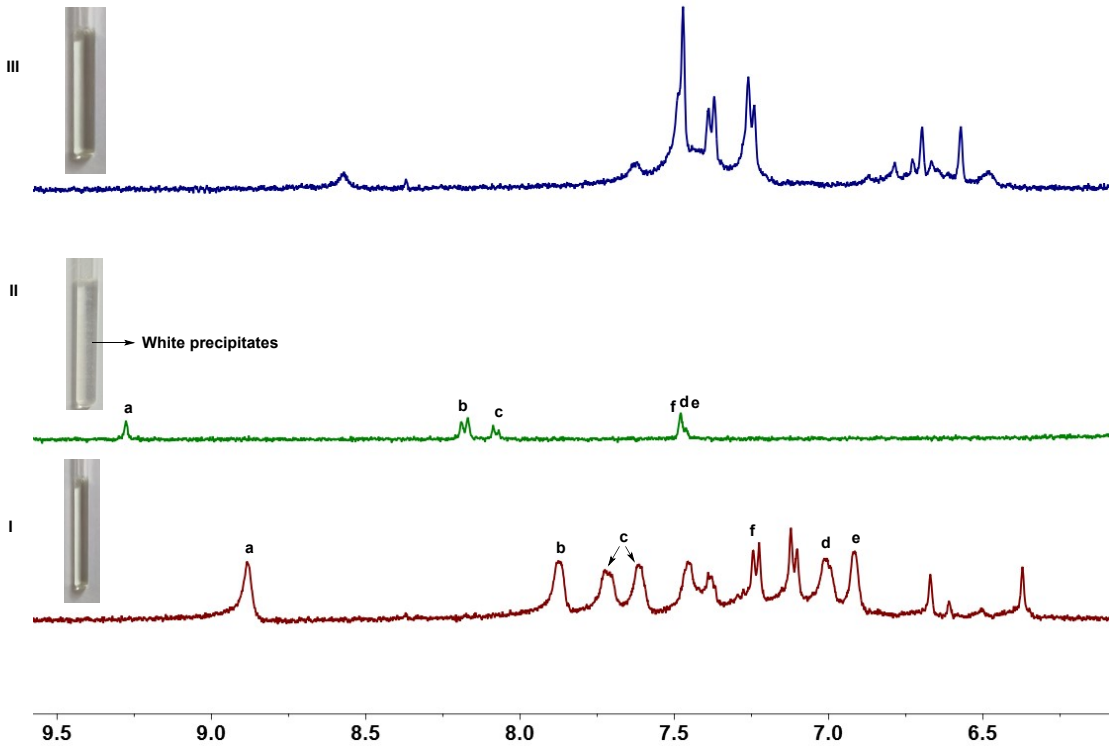

Figure S27. Partial ^{1}H NMR spectra (400 MHz, D_2O, 295 K) and photographs of (I) **1** and 1.0 equiv of **G3**, (b) after addition of 2.0 μL of aqueous DCl solution (20 wt%) to I, and (III) after addition of 1.0 μL of aqueous NaOD solution (40 wt%) to II. $[\mathbf{1}]_0$ = 1.0 mM.

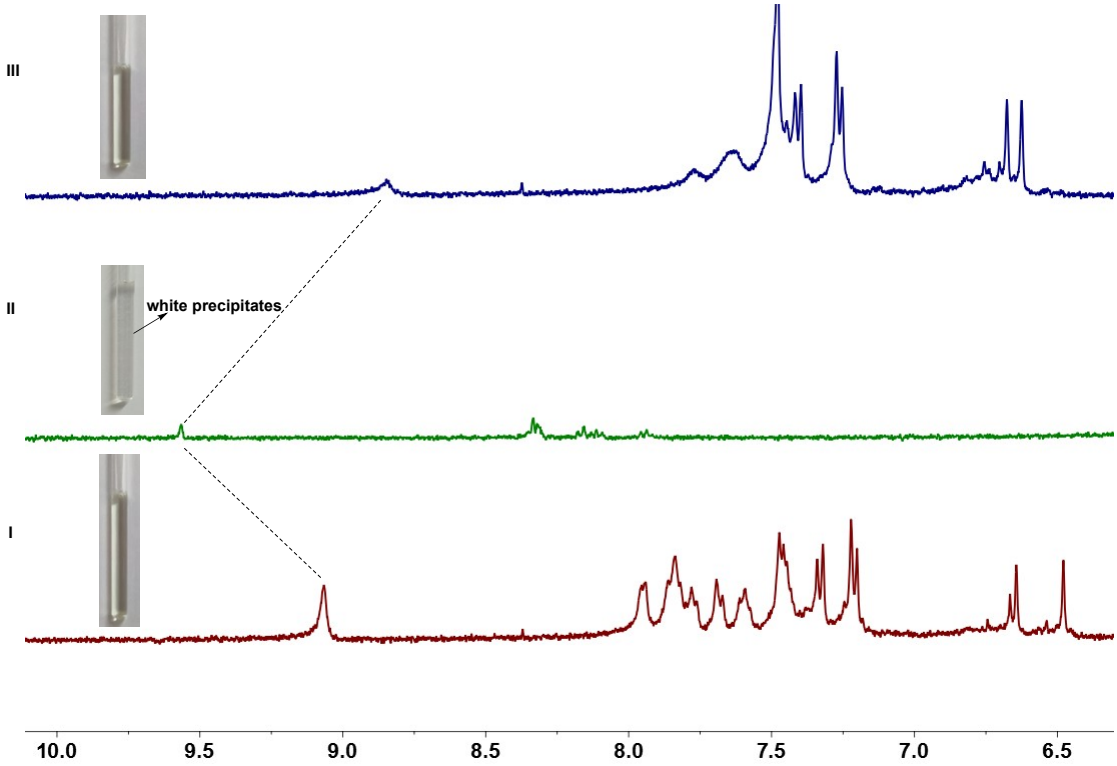

Figure S28. Partial ^{1}H NMR spectra (400 MHz, D_2O, 295 K) and photographs of (I) **1** and 1.0 equiv of **G4**, (b) after addition of 2.0 μL of aqueous DCl solution (20 wt%) to I, and (III) after addition of 1.0 μL of aqueous NaOD solution (40 wt%) to II. $[\mathbf{1}]_0$ = 1.0 mM.

7. ESI MS studies of new compouds and complexes

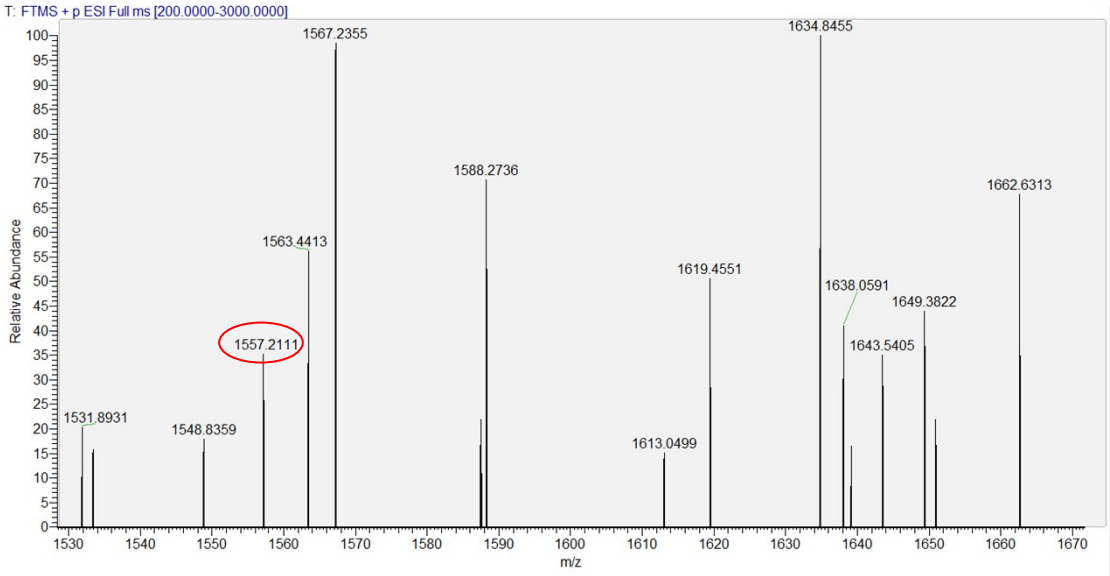

Figure S29. ESI Spectrum of **1**

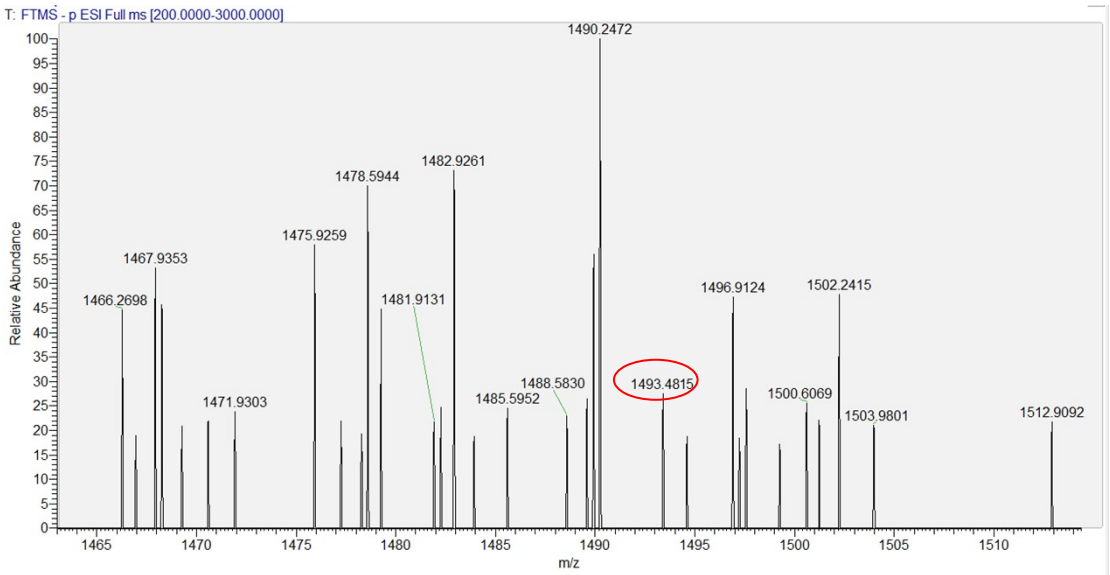

Figure S30. ESI Spectrum of **2**

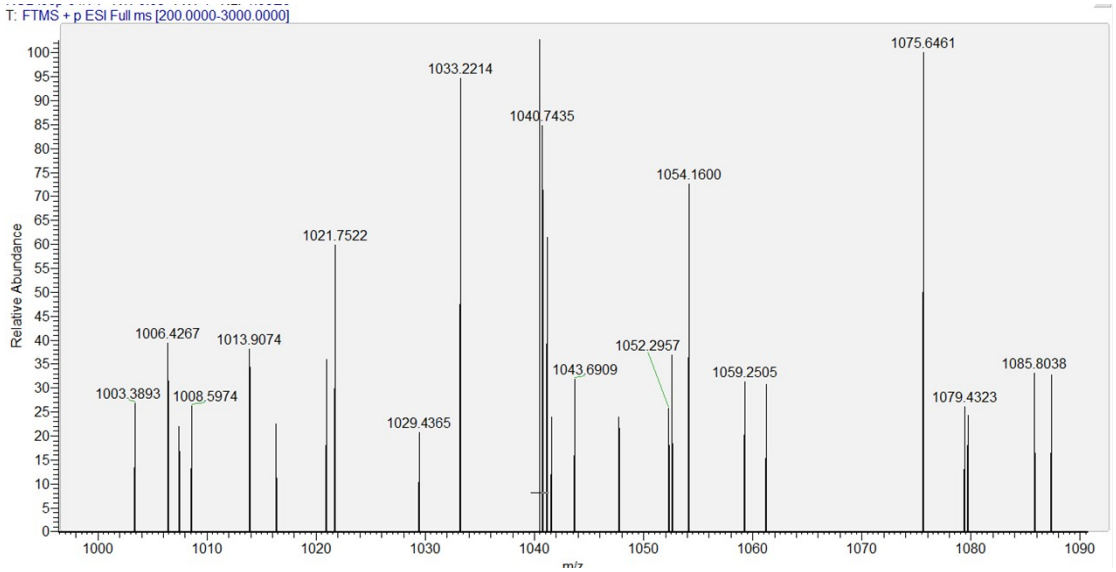

Figure S31. ESI Spectrum of **3**

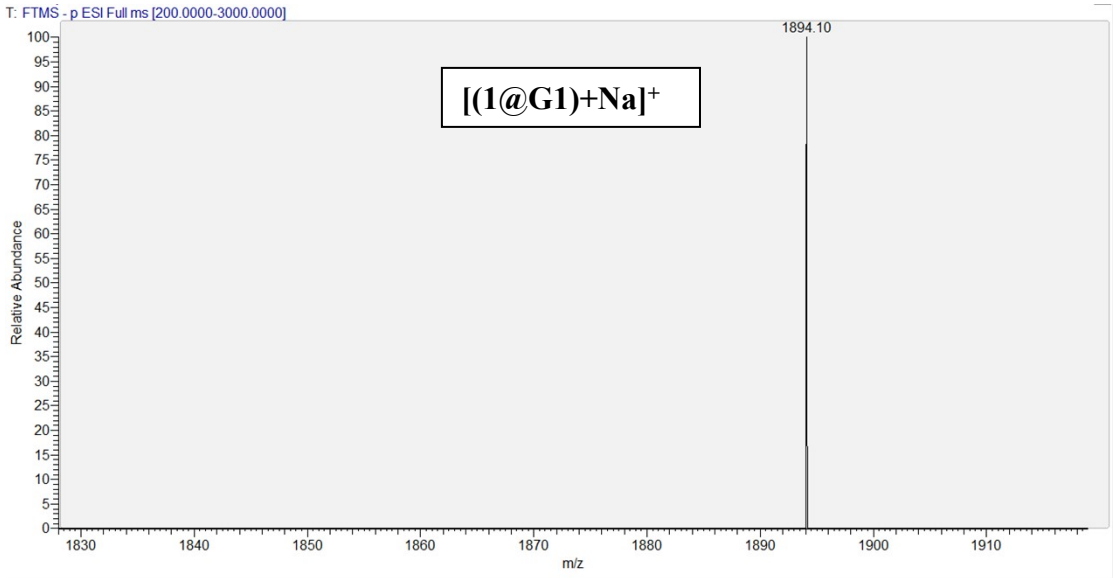

Figure S32. ESI Spectrum of complex **1@G1**

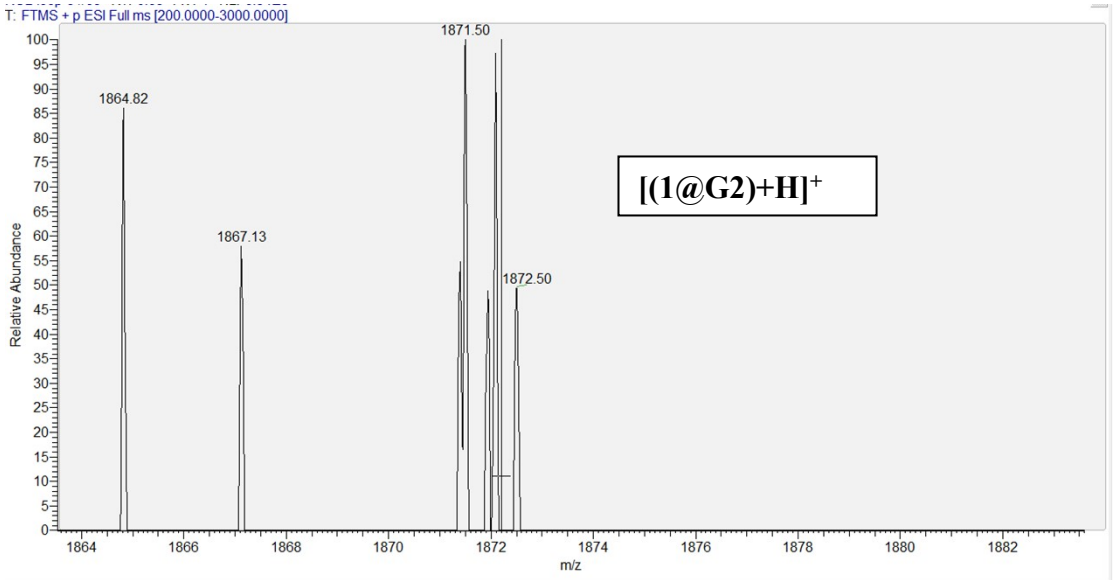

Figure S33. ESI Spectrum of complex **1@G2**

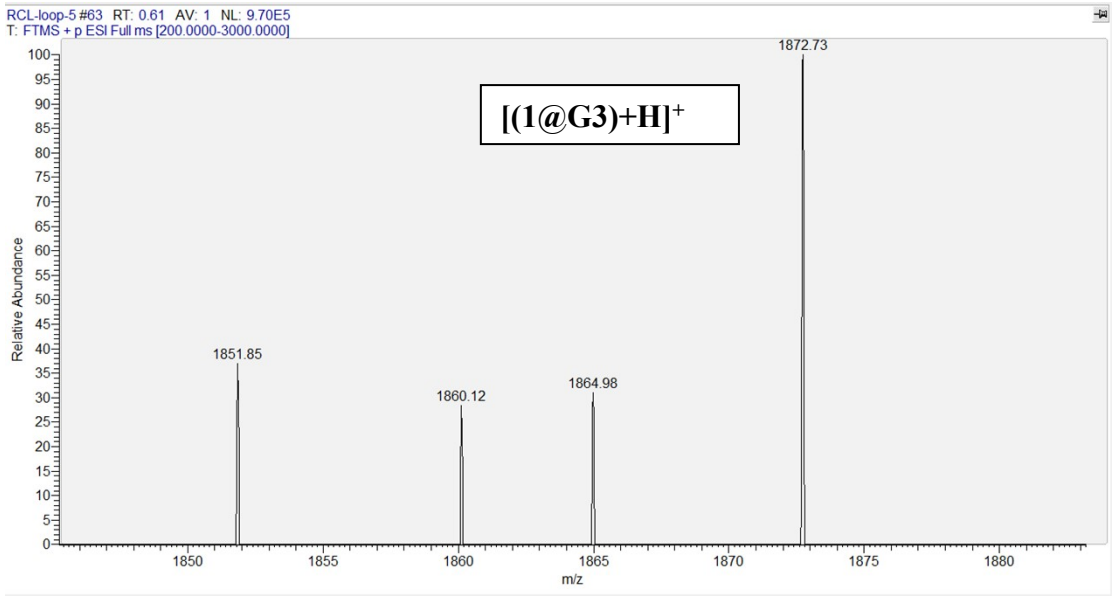

Figure S34. ESI Spectrum of complex **1@G3**

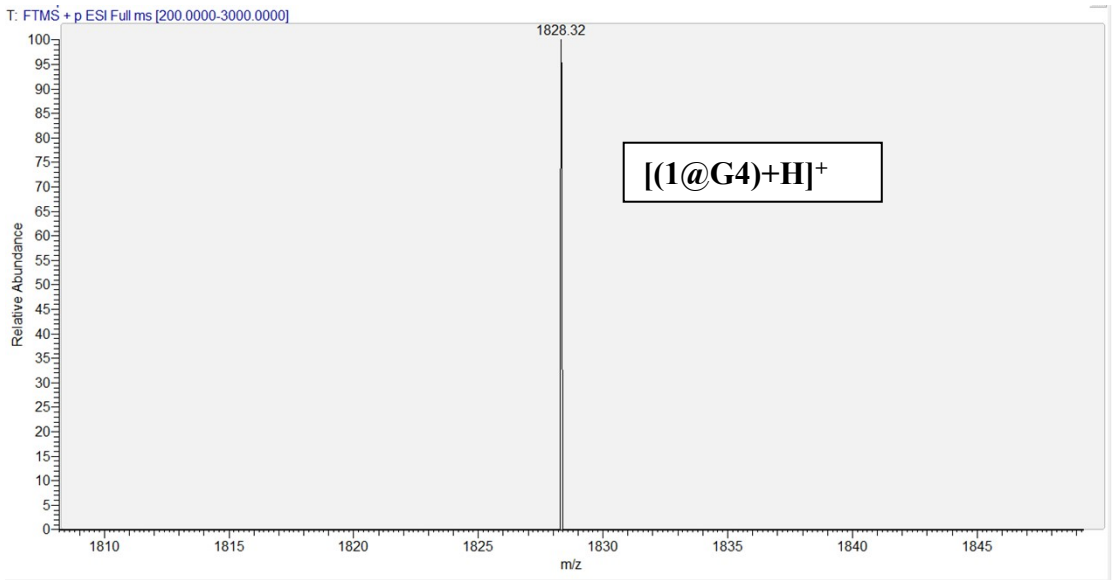

Figure S35. ESI Spectrum of complex **1@G4**

8. Crystal structure data of 3

Crystal data and structure refinement for 11.

Identification code	11
Empirical formula	$C_{72}H_{62}Cl_6O_8$
Formula weight	1267.91
Temperature/K	296.15
Crystal system	monoclinic
Space group	$P2_1/n$
a/Å	10.428(6)
b/Å	30.790(16)
c/Å	11.823(6)
α/°	90
β/°	98.347(5)
γ/°	90
Volume/Å^3	3756(4)
Z	2
ρ_{calc}g/cm^3	1.121

μ/mm^{-1}	0.277
F(000)	1320.0
Crystal size/mm^3	0.13 × 0.12 × 0.09
Radiation	MoKα (λ = 0.71073)
2Θ range for data collection/°	2.646 to 50.052
Index ranges	$-12 \leq h \leq 12$, $-36 \leq k \leq 36$, $-14 \leq l \leq 14$
Reflections collected	32904
Independent reflections	6631 [R_{int} = 0.1200, R_{sigma} = 0.1154]
Data/restraints/parameters	6631/0/392
Goodness-of-fit on F^2	1.018
Final R indexes [I>=2σ (I)]	R_1 = 0.0896, wR_2 = 0.2601
Final R indexes [all data]	R_1 = 0.1900, wR_2 = 0.3254
Largest diff. peak/hole / e $Å^{-3}$	0.57/-0.48